IEEE Access
Multidisciplinary | Rapid Review | Open Access Journal

Received December 3, 2020, accepted December 18, 2020, date of publication December 28, 2020, date of current version January 6, 2021.

*Digital Object Identifier 10.1109/ACCESS.2020.3047674*

# Secrecy Performance of a Multi-NOMA-MIMO System in the UEH Relaying Network Using the PSO Algorithm

**LE THI ANH AND IC PYO HONG, (Member, IEEE)**
Department of Information and Communication Engineering, Kongju National University, Cheonan 31080, South Korea
Corresponding author: Ic Pyo Hong (iphong@kongju.ac.kr)

This research was supported by Basic Science Research Program (2020R1I1A3057142) and the Priority Research Centers Program (2019R1A6A1A03032988) through the National Research Foundation of Korea.

**ABSTRACT** In this paper, we investigate the secrecy performance of the nonorthogonal multiple access (NOMA) system in an untrusted relaying energy harvesting (UEH) network with the multiple-input multiple-output (MIMO) architecture using the maximum ratio transmission (MRT) and maximal ratio combining (MRC) techniques. In this network, a source communicates with users with the help of a relaying network composed of multiple untrusted components using the amplify-and-forward (AF) protocol. These untrusted relay nodes are equipped with a single antenna and employ the power-splitting (PS) protocol to harvest energy from received signals. Moreover, to improve the secrecy outage performance and protect the confidential information from the untrusted relaying network, the source acts as the jammer to generate artificial noise (AN). To evaluate the secrecy performance of each user and the overall system, we derive the closed-form expressions of the secrecy outage probability (SOP) over the Rayleigh fading channels and use a Monte Carlo simulation to verify the accuracy of these analytical results. Moreover, to analyze the secrecy data rate, the maximization problem of the sum secrecy rate (SSR) of the system is solved by applying the particle swarm optimization (PSO) algorithm based on power allocation (PA). These results are also validated with the optimal exhaustive search method. Furthermore, we compare the MIMO/NOMA and MIMO/OMA systems and examine the effects of various system parameters to characterize the secrecy effectiveness of both systems.

**INDEX TERMS** Multiple-input multiple-output, multiple nonorthogonal multiple access, untrusted relaying energy harvesting network, secrecy sum rate, artificial noise; particle swarm optimization.

## I. INTRODUCTION

With the rapid development of wireless communication technology, fifth-generation (5G) wireless networks have already been launched in many countries and will be fully deployed worldwide in 2021. Recently, the research community has shifted its focus towards the high requirements for future networks known as beyond 5G (B5G) and sixth-generation (6G) networks that are based on the trends of the previous generations will incorporate new technologies and provide new services. The most important requirements for B5G and 6G wireless networks are the ability to handle large volumes of data, massive connectivity, ultra-low latency, and high security [1]–[3]. To accommodate the high demands of B5G and 6G, many advanced wireless technologies will be developed such as new multiple-access, MIMO, terahertz communications, visible light communication, and EH and UAV techniques. Moreover, due to the scale, density, and complexity of the future networks, integration of these wireless techniques and artificial intelligence (AI) will solve optimization and dynamic application problems while traditional optimization algorithms with complicated mathematical models such as Lagrangian duality and gradient methods will no longer be suitable [4].

The associate editor coordinating the review of this manuscript and approving it for publication was Tao Wang.

### A. BACKGROUND

The nonorthogonal multiple access (NOMA) technique has been evaluated as an optimal solution for the incoming 5G and B5G communication networks because NOMA can meet the requirements of future networks, such as high throughput, low latency, and massive connectivity. The outstanding

advantages of the NOMA approach compared to the conventional orthogonal multiple-access (OMA) techniques with high spectral and capacity efficiencies and user fairness are considered in [5]–[7]. There are two main categories of NOMA technique: power domain NOMA (PDNOMA) and code domain NOMA [8]. In this paper, we focus on PDNOMA. In contrast to traditional OMA, multiple users in PDNOMA are served at the same time, frequency, and code, and their signals are multiplexed by using different power levels based on the channel quality [9]. Specifically, in PDNOMA, users under weaker channel conditions will be allocated more transmission power, and successive interference cancellation (SIC) at the receiver is employed to help detect the desired signal. Henceforward, we refer to PD-NOMA system in this paper simply as the NOMA system. In [10], the authors provide a detailed description of NOMA for 5G networks, including solutions, challenges, opportunities, and future research trends. In particular, they discussed the characteristics of system settings, decoding strategies, system asymmetries, and power allocation (PA) and comparisons among the existing cooperative relay architectures.

In addition to the studies on the effectiveness of NOMA, previous work has emphasized the combination of NOMA with many earlier well-known techniques that have been employed to improve the performance of communication systems. Specifically, [11], [12] analyzed the system performance of a downlink cooperative NOMA scheme with an AF relay, and based on the comparison of NOMA with OMA, it was concluded concluded that NOMA offers better spectral efficiency and user fairness. The application of NOMA to a cognitive radio system with a novel CSS framework was proposed to improve spectral efficiency in [13]. Additionally, the integration of NOMA with cognitive radio into a holistic system for more intelligent spectrum sharing was presented in [14]. Moreover, the applications of multiple-input multiple-output (MIMO) to NOMA have been considered in several reported studies. For instance, in [15], multiple antenna techniques in NOMA networks were exploited with an emphasis on investigating the rate region in which two popular multiple antennas aided NOMA architectures and the performance of MIMO-NOMA was compared to that of MIMO-OMA. In [16], the performance of MIMO/NOMA was also investigated when multiple users are grouped in a cluster, exploring both the sum channel capacity and ergodic sum capacity and the results were compared with the results obtained using MIMO/OMA .

Additionally, obtaining reduced energy consumption in order to prolong the lifetime of relay nodes is an important issue in the development of cooperative networks. Energy harvesting (EH) using radio-frequency signals is a potential solution to increase the node lifetime, reduce the need for replacing and recharging the batteries of wireless devices, and maintaining network connectivity [17]–[19]. Many published studies have investigated the system performance of a wireless network using the EH method for power harvesting from RF signals. In particular, in a cooperative EH network, relay nodes with EH capabilities can solve the energy supply problem and expand the range of applications to perform information forwarding in a restricted transmission range [20]–[22]. In another study [23], the authors also considered an AF relaying network in which an energy-constrained relay node collects the energy from the received RF signal and uses the harvested energy to forward the source information to the destination. Moreover, two relaying protocols were proposed, namely, the power splitting (PS) protocol and time switching (TS) protocols to enable wireless EH and information processing at the relay.

Later, to exploit the advantage of the above techniques for wireless networks, many studies investigated combining these methods into a network system. For instance, cooperative NOMA with the simultaneous wireless information and power transfer (SWIPT) is an attractive combination for obtaining high capacities and power efficiencies for wireless communication [24], [25]. Moreover, [26] considered multi-antenna beam-forming in an EH-NOMA network that delivered information and energy separately in fractional times, enabling EH by simple devices. These studies formulated two important problems of throughput max-min optimization and energy efficiency (EE) maximization under power constraint and EH constraints at the nearly-located users. Moreover, the EE optimization for NOMA with SWIPT supporting the functionality of the Internet of Things and the massive machine-type communication scenarios was investigated in [27].

A key aspect of the future communication network is security and the development of methods for enhancing the secrecy transmission in the wireless medium. Because of the broadcast of wireless communication, information transmitted from transceivers to the receiver can be overheard by eavesdroppers, leading to significant and troubling security issues. One of the research directions in the studies of security in wireless communication is the exploitation of jamming signals that consist of artificial noise to improve the security of the system by combating eavesdropping attacks [28], [29]. Recently, the secrecy performance of the NOMA system has been recognized as an important research topic [30]–[32]. Additionally, in [33] the authors considered the secrecy outage performance of a multiple-relay assisted NOMA network over Nakagami-$m$ fading channels and proposed three relay selection schemes. Some researchers have considered the secrecy performance for cooperative systems with an untrusted relaying network in which the relay nodes act as both helpers that assist the transmission from the source to destination and potential eavesdroppers that attempt to overhear the confidential information [34], [35]. Furthermore, [36] considered the effective secrecy rate (ESR) of the down-link NOMA network with one base station, multiple single-antenna NOMA users, and an internal or external eavesdropper.

Moreover, in NOMA systems with SWIPT, the problem of optimization of system parameters, particularly of power

allocation (PA) to each user, is one of the most important problems that must be addressed to improve the system performance [27], [33], [37], [38]. In particular, [37] designed a power allocation algorithm with multiple constraints in which a PA for NOMA as a mixed-integer programming problem was formulated. In this work, the energy efficiency optimization problem was solved using Lyapunov optimization. While the study of the NOMA system with SWIPT was proposed, [38] considered the secrecy sum-rate maximization of the NOMA system under the constraints on the individual user's minimum rate and harvested power. Furthermore, cooperative NOMA with SWIPT was also studied in [27], where power allocation and time switching controls for the energy efficiency optimization in NOMA with SWIPT were investigated. In this work, the authors developed a dual-layer iterative resource allocation algorithm and provided power allocation and TS control for possible implementation in practical SWIPT-enabled NOMA systems. Unlike the the approach of heavy mathematical analysis for optimization problems used in the traditional optimization methods, artificial intelligence (AI) techniques, particularly swarm intelligence (SI) techniques, can be used to perform global optimization and address nonlinear complex problems [39]. Particle swarm optimization (PSO) with the very simple calculation is one of the SI algorithms that can be used to find approximate solutions to extremely difficult and complex problems with advanced capabilities in terms of self-adaptability, robustness, and searchability [40], [41]. Previous studies [42]–[45] have applied the PSO algorithm to improve the performance of wireless networks.

### B. MOTIVATION AND CONTRIBUTIONS

To the best of our knowledge, there are no reports in the literature on the investigations of secrecy outage performance for a cooperative NOMA/MIMO system using MRT/MRC with imperfect SIC in the multiple UEH relaying network employing PS architecture and multiple destination users. In addition, the application of a modern heuristic PSO algorithm for the improvement of secrecy performance of the NOMA system is still limited. Thus, in this paper, we propose the use of NOMA/MIMO in UEH relaying network and also consider the secrecy performance in combination with the PSO algorithm where PSO solves the maximization SSR problem based on PA with multiple constraint conditions. In particular, in our proposed system, the source S acts as a transceiver transmitting the destination signals and a jammer broadcasting the jamming signal to generate artificial noise in order to reduce the loss of user information and improve the secrecy capacity. Moreover, the UEH relay node with a single antenna also acts as both a helper assisting in forwarding the received signals from S to the destinations and as potential eavesdroppers trying to overhear the confidential information. Accordingly, the source S node is equipped with multiple antennas and communicates with multiple antennas users via a multiple AF-UEH relaying network. The main contributions of our study are as follows:

- (1) We first derive the analytical expression of the secrecy outage probability (SOP) for each user of a multi-MIMO/NOMA scheme with the untrusted AF-EH relaying network employing the PS protocol. The accuracy of the analytical results is verified using Monte Carlo simulations.
- (2) We investigate the effects of various system parameters such as the numbers of the antenna and relay nodes, power allocation coefficients, power-splitting ratio, jamming signal, and the imperfect SIC on the system performance.
- (3) We solve the SSR maximization problem with multiple constraints for the multi-MIMO/NOMA system based on the power allocation that uses the PSO algorithm. Moreover, the optimal PA is applied to evaluate the SOP in comparison with other cases.
- (4) The analysis of the secrecy outage performance and secrecy data rate are performed for both the MIMO/NOMA and MIMO/OMA system to conduct a comparison of the relative efficiencies. Furthermore, we demonstrated that the use of the Golden Section Search method to find the optimal value of the power-splitting factor in the EH technique improves the secrecy performance.

The rest of this paper is organized as follows: the system model and signal transmission are described in Section 2; next, the analysis of secrecy performance is presented in Section 3; the simulation results and discussion are given in Section 4; the conclusions are summarized in Section 5; and finally, the proofs of the mathematical problems are given in the Appendixes.

*Notation*: $\|.\|$ is the Frobenius norm; $\mathcal{CN}(0, \varpi)$ is a complex Gaussian distribution with zero mean and variance $\omega$; $\Gamma(.)$ is the gamma function [ [50],Eq. (8.310.1)]; $\mathcal{F}_v(.)$ is the $v$-th order modified Bessel function [ [50],Eq.(8.407.1)] and $\binom{k}{i} = \frac{k!}{i!(k-i)!}$.

## II. SYSTEM MODEL AND SIGNAL TRANSMISSION

### A. SYSTEM MODEL

We consider a system model of the downlink NOMA/MIMO network with UEH relays that is presented in Figure 1. In our proposed system, the source $S$ and users are equipped with multiple antenna, respectively $N_0$, $N_1$ and $N_2$ antennas, with a cluster of $K$ single-antenna UEH relay nodes denoted by $R_k$ ($k = 1, \ldots, K$). These $K$ UEH relays act as both the AF relay to forward information from $S$ to the users and as the eavesdroppers that try to overhear confidential information. Additionally, the $K$ relay nodes are assumed to be located close to each other, forming a relay cluster; hence, the distances between the relays are very small compared to the distances of the $S$-$R$ and $R$-user links [18]. Thus, we can assume that distances from source to relays are equivalent, $d_{01} \simeq d_{02} \simeq \ldots \simeq d_{0k} \simeq \ldots \simeq d_{0K} = d_0$. To exploit the benefit of using multiple antennas, $S$ and the users apply MRT and MRC, respectively. Moreover, only the best relay $R_b$

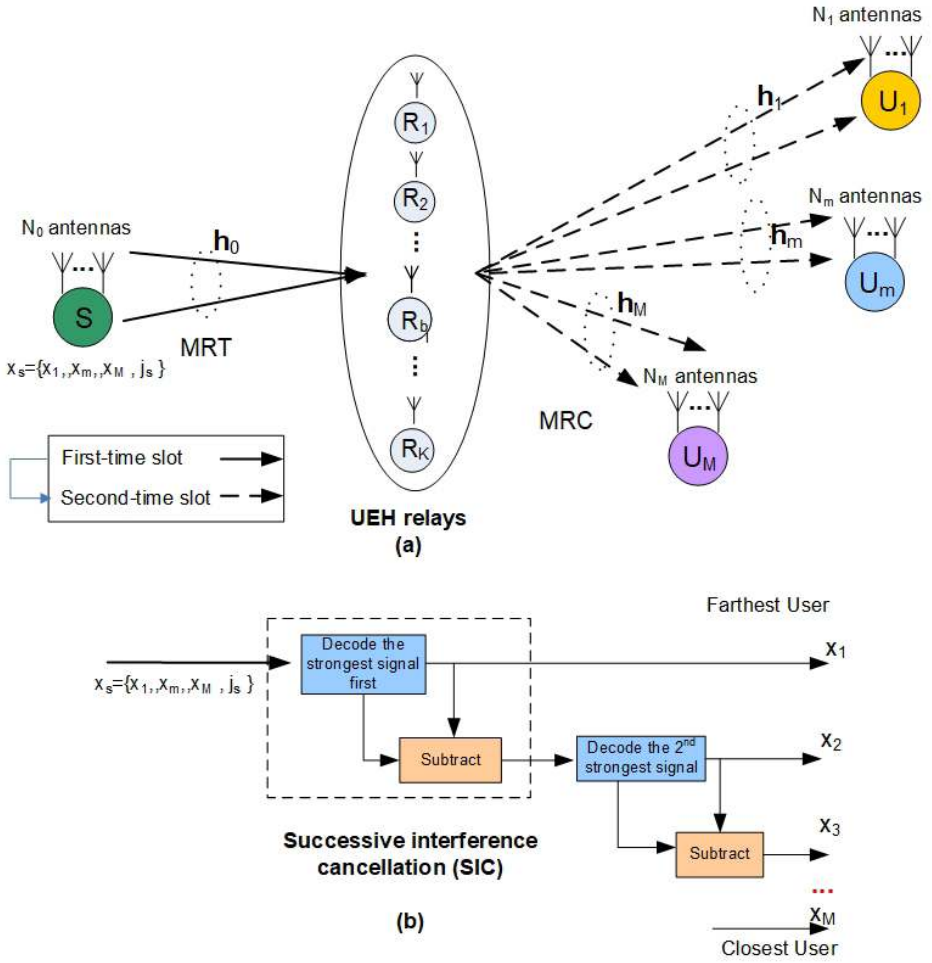


**FIGURE 1.** The system model and SIC.

selected to help the $S$-to-users transmission from the $K$ UEH relays. $R_b$ applies the PS architecture to harvest energy from the source signal using a power splitting ratio $\rho$ $(0 < \rho < 1)$ of the received signal power for energy harvesting and $(1-\rho)$ of the signal power for information processing.

Throughout this paper, we assume that (i) there are no direct links between $S$ and users; (ii) the channels are identically and independently distributed Rayleigh block-fading channels, and thus the channel gains are exponential random variables (RVs); (iii) the processing power required by the transmit/receive circuitry at the relay is negligible compared to the power used for signal transmission from the relay to the users [24] (iv) the local channel state information (CSI) is assumed at $R$, and global CSI is assumed at $S$ and the users; (v) the distances of $S-U_1$,$S-U_2$,...$S-U_M$ are denoted as $d_1, d_2,\ldots, d_M$, respectively and $d_1 > d_2 >, \ldots, > d_M$ ; and, (vi) the AN cancellation at users is perfect and the AN signal is perfectly known to the users but not to the UEH relay [32], [33].

We denote $\mathbf{h}_{0,k} = \left[h_{0,k,1}, \ldots, h_{0,k,N_0}\right]$, $\mathbf{h}_{1,k} = \left[h_{1,k,1}, \ldots, h_{1,k,N_1}\right]^T, \ldots, \mathbf{h}_{m,k} = \left[h_{m,k,1}, \ldots, h_{m,k,N_2}\right]^T$,.. and $\mathbf{h}_{M,k} = \left[h_{M,k,1}, \ldots, h_{M,k,N_2}\right]^T$ as the channel vectors of the $S-R_k, R_k-U_1, \ldots, R_k-U_m$,... and $R_k-U_M$ links, respectively. The elements of these channel vectors follow identically and independently distributed channel gains where $m = 0, 1, 2, \ldots, M$, $i = 1, 2, \ldots, N_m$ and $d_m$ is the normalized distance between $S-R_k$, $R_k-U_1$, ..., $R_k-U_m$,... and $R_k-U_M$, and $v$ is the path loss exponent. The probability density function (PDF) and cumulative distribution function (CDF) of $g_{m,k,i}$ are obtained as $f_{g_{m,k,i}}(x) = e^{-\frac{x}{\lambda_m}}/\lambda_m$, and $F_{g_{m,k,i}}(x) = 1 - e^{-\frac{x}{\lambda_m}}$ respectively.

### B. SIGNAL TRANSMISSION

In this paper, to determine the best relay $R_b$, we employ MRT that is based on partial relay selection on the first-hop CSIs. The strategy of MRT is described as follows:

$$R_b = \arg \max_{1 \le k \le K} \left\{ \left\| \mathbf{h}_{0,k} \right\|^2 \right\}. \quad (1)$$

In the MRT scheme, to maximize the signal-to-interference noise ratio (SINR) at $R_b$, $S$ employs a transmit beamforming vector $\mathbf{w}_s = \mathbf{h}_{0,b}^{\dagger} / \left\| \mathbf{h}_{0,b} \right\|$ to its signal $x$ before transmitting $\mathbf{w}_s x$ to users, where $\mathbf{h}_{0,b} = \left[h_{0,b,1}, \ldots, h_{0,b,N_0}\right]$ is a channel vector of the $S-R_b$ link and $E\{xx^*\} = 1$. The PDF and CDF

of $\left\|\mathbf{h}_{m,k}\right\|^2$ are respectively given by

$$f_{\left\|\mathbf{h}_{m,k}\right\|^2}(x) = \frac{x^{N_m-1}}{\Gamma(N_m)\lambda_m^{N_m}} e^{-\frac{x}{\lambda_m}}, \tag{2a}$$

$$F_{\left\|\mathbf{h}_{m,k}\right\|^2}(x) = 1 - e^{-\frac{x}{\lambda_m}} \sum_{j=0}^{N_m-1} \frac{1}{j!}\left(\frac{x}{\lambda_m}\right)^j. \tag{2b}$$

By defining $g_{0,b} \triangleq \max\limits_{1\le k\le K}\left\{\left\|\mathbf{h}_{0,k}\right\|^2\right\}$, the PDF and CDF of $g_{0,b}$ are described as

$$f_{g_{0,b}}(x) = K\frac{x^{N_0-1}}{\Gamma(N_0)\lambda_0^{N_0}} e^{-\frac{x}{\lambda_0}}\left(1 - e^{-\frac{x}{\lambda_0}}\sum_{j=0}^{N_0-1}\frac{1}{j!}\left(\frac{x}{\lambda_0}\right)^j\right)^{K-1} \tag{3a}$$

$$F_{g_{0,b}}(x) = \left(1 - e^{-\frac{x}{\lambda_0}}\sum_{j=0}^{N_0-1}\frac{1}{j!}\left(\frac{x}{\lambda_0}\right)^j\right)^K. \tag{3b}$$

In the first time slot, after selecting the best UEH relay, the superimposed mixture of the signals intended for the informative signals of $U_1$, $U_2$,..., $U_i$, ..., $U_M$ and AN is simultaneously transmitted to $R_b$, as described by

$$x = \sum_{i=1}^{M}\sqrt{P_i}x_i + \sqrt{P_{js}}j_s. \tag{4}$$

where $P_i$ is the power allocated to user $i$, $P_1 > P_2 > \ldots > P_M$ and $P_{js}$ is the power for the jamming signal or AN.

The received signal at the best relay is provided by

$$y_{R_b} = \sum_{i=1}^{M}\sqrt{P_i}\mathbf{h}_{0,b}\mathbf{w}_s x_i + \sqrt{P_{js}}\mathbf{h}_{0,b}\mathbf{w}_s j_s + n_R^a. \tag{5}$$

where $n_R^a$ is the antenna additive white Gaussian noise (AWGN) at $R_b$ and $n_R^a \sim CN\left(0, \sigma_{R_b}^{2(a)}\right)$.

Based on equation (5), the instantaneous SINRs at $R_b$ can be expressed as

$$\gamma_{x_1}^{R_b} = \frac{P_1\left\|\mathbf{h}_{0,b}\right\|^2}{\sum\limits_{m=2}^{M}P_m\left\|\mathbf{h}_{0,b}\right\|^2 + P_{js}\left\|\mathbf{h}_{0,b}\right\|^2 + \sigma_{R_b}^2}, \tag{6}$$

$$\gamma_{x_2}^{R_b} = \frac{P_1\left\|\mathbf{h}_{0,b}\right\|^2}{\left(P_1 + \sum\limits_{m=3}^{M}P_m\right)\left\|\mathbf{h}_{0,b}\right\|^2 + P_{js}\left\|\mathbf{h}_{0,b}\right\|^2 + \sigma_{R_b}^2}, \tag{7}$$

$$\ldots..$$

$$\gamma_{x_m}^{R_b} = \frac{P_m\left\|\mathbf{h}_{0,b}\right\|^2}{\left(\sum\limits_{l=1}^{m-1}P_l + \sum\limits_{q=m+1}^{M}P_q\right)\left\|\mathbf{h}_{0,b}\right\|^2 + P_{js}\left\|\mathbf{h}_{0,b}\right\|^2 + \sigma_{R_b}^2}, \tag{8}$$

$$\ldots..$$

$$\gamma_{x_M}^{R_b} = \frac{P_m\left\|\mathbf{h}_{0,b}\right\|^2}{\sum\limits_{q=m+1}^{M-1}P_m\left\|\mathbf{h}_{0,b}\right\|^2 + P_{js}\left\|\mathbf{h}_{0,b}\right\|^2 + \sigma_{R_b}^2}. \tag{9}$$

According to [25], in the PS protocol, at relay $R_b$, the received signal, $y_{R_b}$, in (5) is split into two parts, including $\sqrt{\rho}y_{R_b}^{PS}$ for energy harvesting and $\sqrt{1-\rho}y_{R_b}^{PS}$ information processing that can be respectively expressed as

$$\sqrt{\rho}y_{R_b}^{PS} = \sum_{i=1}^{M}\sqrt{\rho P_i}\mathbf{h}_{0,b}\mathbf{w}_s x_i + \sqrt{\rho P_{js}}\mathbf{h}_{0,b}\mathbf{w}_s j_s + \sqrt{\rho}n_R^a, \tag{10}$$

$$\sqrt{1-\rho}y_{UR_b}^{PS} = \sum_{i=1}^{M}\sqrt{(1-\rho)P_i}\mathbf{h}_{0,b}\mathbf{w}_s x_i + \sqrt{(1-\rho)P_{js}}\mathbf{h}_{0,b}\mathbf{w}_s j_s + \sqrt{1-\rho}n_R^a. \tag{11}$$

For convenience of the calculation, we define $g_0$ as $g_0 = \left\|\mathbf{h}_{0,b}\right\|^2$. The energy EH harvested from the received signal at $R_b$ is given by

$$E_{EH}^{PS} = \mu\frac{\rho\left(\sum\limits_{m=1}^{M}P_m + P_{js}\right)g_0 T}{2}. \tag{12}$$

where $T/2$ is half of the transmission time block, and $\mu$ is the energy conversion efficiency such that $0 < \mu \le 1$.

The received RF signal is sampled by the RF-to-baseband conversion units. Hence, the input signal of the information receiver of $R_b$ in the PS protocol is given by

$$y_R^{c(PS)} = \sum_{i=1}^{M}\sqrt{(1-\rho)P_i}\mathbf{h}_{0,b}\mathbf{w}_s x_i + \sqrt{(1-\rho)P_{js}}\mathbf{h}_{0,b}\mathbf{w}_s j_s + \underbrace{\sqrt{1-\rho}n_R^a + n_R^c}_{n_R}. \tag{13}$$

where $n_R^c$ is the conversion additive white Gaussian noise (AWGN) at $R_b$ with $n_R^c \sim \mathcal{CN}(0, \sigma_{n_R^c}^2)$, and $n_R = \sqrt{1-\rho}n_R^a + n_R^c$ denotes the overall AWGN at $R_b$, and $\sigma_{R_b}^2 = (1-\rho)\sigma_{R_b}^{2(a)} + \sigma_{n_R^c}^2$.

In the second time slot, by using the AF protocol, the remaining signal was broadcast by the best relay node to the users before amplifying the $\sqrt{1-\rho}y_{R_b}^{PS}$ signal with gain

$$G = \left((1-\rho)\left(\sum_{m=1}^{M}P_m + P_{js}\right)g_0 + \sigma_R^{2(PS)}\right)^{-1}.$$

As a result, the received signals at $U_m$ can be expressed as

$$y_{U_m}^{PS} = \sum_{m=1}^{M}\sqrt{GP_r P_m(1-\rho)}\mathbf{h}_{0,b}\mathbf{h}_{bm}\mathbf{w}_s x_m + n_{U_m} + \sqrt{GP_r P_{js}(1-\rho)}\mathbf{h}_{0,b}\mathbf{h}_{bm}\mathbf{w}_s j_s + \sqrt{GP_r}\mathbf{h}_{bm}n_R^{PS}. \tag{14}$$

where $P_r = 2E_{EH}^{PS}/T$.

The received signals of $U_m$ users after MRC are respectively given as

$$x_{U_m}^{PS} = \sum_{m=1}^{M} \sqrt{GP_r P_m (1-\rho)}\mathbf{h}_{0,b}\mathbf{h}_{bm}\mathbf{w}_s\mathbf{w}_{U_m}x_m + \mathbf{w}_{U_m}n_{U_m} + \sqrt{GP_r P_{js} (1-\rho)}\mathbf{h}_{0,b}\mathbf{h}_{bm}\mathbf{w}_s\mathbf{w}_{U_m}j_s + \sqrt{GP_r}\mathbf{h}_{bm}\mathbf{w}_{U_m}n_R^{PS}. \quad (15)$$

where $\mathbf{w}_{U_m} = \mathbf{h}_{bm}^{\dagger}/\|\mathbf{h}_{bm}\|$ is the weight vector for the MRC.

Because $U_m$ can eliminate the AN in (15), $x_{U_m}^{PS}$ can be rewritten as

$$x_{U_m}^{PS} = \sum_{m=1}^{M} \sqrt{GP_r P_m (1-\rho)}\mathbf{h}_{0,b}\mathbf{h}_{bm}\mathbf{w}_s\mathbf{w}_{U_m}x_m + \sqrt{GP_r}\mathbf{h}_{bm}\mathbf{w}_{U_m}n_R^{PS} + \mathbf{w}_{U_m}n_{U_m}. \quad (16)$$

Let denotes $g_m = \|\mathbf{h}_{bm}\|^2$. From (16), the instantaneous end-to-end SINRs at $U_m$ can be evaluated as

$$\gamma_{x_1}^{U_m} = \frac{P_1\theta_1 g_0 g_m}{\sum_{m=2}^{M} P_m\theta_1 g_0 g_m + \theta_2 g_m + 1}, \quad (17)$$

$$\gamma_{x_2}^{U_m} = \frac{P_2\theta_1 g_0 g_m}{\left(\varepsilon P_1 + \sum_{3}^{M} P_m\right)\theta_1 g_0 g_m + \theta_2 g_m + 1}, \quad (18)$$

$$\gamma_{x_m}^{U_m} = \frac{P_m\theta_1 g_0 g_m}{\left(\varepsilon \sum_{l=1}^{m-1} P_l + \sum_{q=m+1}^{M} P_q\right)\theta_1 g_0 g_m + \theta_2 g_m + 1}, \quad (19)$$

$$\gamma_{x_M}^{U_m} = \frac{P_M\theta_1 g_0 g_m}{\varepsilon \sum_{m=1}^{M-1} P_m\theta_1 g_0 g_m + \theta_2 g_m + 1}. \quad (20)$$

Here $\theta_1 = \frac{\mu\rho}{\sigma_{U_m}^2}$, $\theta_2 = \frac{\mu\rho\sigma_{R_b}^2}{(1-\rho)\sigma_{U_m}^2}$, and $\varepsilon$ is the cancellation error term that represents the remaining portion of the canceled message signal in the NOMA model.

## III. SECRECY PERFORMANCE ANALYSIS

In this section, we analyze the secrecy performance at each user and for the overall system using the proposed model including the secrecy outage probability (SOP) performance and sum secrecy rate. In NOMA, evaluation of the SOP and SSR of the system is performed by examining the security transmission performance of all destination nodes in which each user must be satisfied that its instantaneous secrecy rate $R_{\text{sec}}^{U_m}$ is at least a given threshold value $R_{th}$. $U_m$ with the secrecy rate $R_{\text{sec}}^{U_m}$ [46] that can be calculated as

$$R_{\text{sec}}^{U_m} = \left[R_{x_m}^{U_m} - R_{x_m}^{R_b}\right]^+. \quad (21)$$

### A. THE SOP AT $U_m$

According to [46], [47], the secrecy outage probability is defined as the probability of the instantaneous secrecy rate (in Eq. 21) falling below the given secrecy data rate. In a NOMA system, because of the SIC principle, $U_m$ decodes the strongest signal $x_1$ first and treats other weaker signals as noise; this action is performed until a desired signal $x_m$ is achieved. In fact, if the stronger signals are incorrectly decoded, the probability to correctly decode symbol $x_m$ is approximately zero. The cancellation error term $\varepsilon$ represents the remaining portion of the canceled message signal. In the proposed model, SIC is absent at the relays; thus, the SOP at $U_m$ occurs in some cases as: (1) $U_m$ successfully decodes the stronger signals of $x_1$, $x_2$, .., $x_{m-1}$ and the secrecy rate at $U_m$ is smaller than a given target secrecy data rate ($R_{th}$); (2) $U_m$ cannot decode the stronger signals and in the fact $U_m$ also cannot detect the signal of $x_m$. Therefore, the SOP can be expressed as

$$SOP_m = 1 - \Pr\left[\begin{matrix}\gamma_{x_1}^{U_m} > \gamma_0, \gamma_{x_2}^{U_m} > \gamma_0, \ldots, \\ \gamma_{x_{m-1}}^{U_m} > \gamma_0, R_{\text{sec}}^{U_m} > R_{th}\end{matrix}\right]. \quad (22)$$

Here, $\gamma_0$ is a threshold at which the user can decode its signal successfully, and $\gamma_0 = 2^{R_0} - 1$ with $R_0$ is a given target data rate.

Substituting the equations (6,7,8,9) and (17,18,19,20) into (22), we obtain

$$\begin{aligned} SOP_m &= 1 - \Pr \\ &\times \left[\begin{matrix} \frac{P_1\theta_1 g_0 g_m}{\sum_{m=2}^{M} P_m\theta_1 g_0 g_m + \theta_2 g_m + 1} > \gamma_0, \\ \frac{P_2\theta_1 g_0 g_m}{\left(\varepsilon P_1 + \sum_{3}^{M} P_m\right)\theta_1 g_0 g_m + \theta_2 g_m + 1} > \gamma_0 \\ , \ldots, \\ \frac{P_{m-1}\theta_1 g_0 g_m}{\left(\varepsilon \sum_{l=1}^{m-2} P_l + \sum_{q=m}^{M} P_q\right)\theta_1 g_0 g_m + \theta_2 g_m + 1} > \gamma_0, \\ \frac{P_m\theta_1 g_0 g_m}{\left(\varepsilon \sum_{l=1}^{m-1} P_l + \sum_{q=m+1}^{M} P_q\right)\theta_1 g_0 g_m + \theta_2 g_m + 1} > \gamma_{th} \end{matrix}\right] \\ &= 1 - A. \end{aligned} \quad (23)$$

here, $\gamma_{th} = 2^{R_{th}} + \frac{2^{R_{th}} P_m}{\left(\sum_{l=1}^{m-1} P_l + \sum_{q=m+1}^{M} P_q\right) + P_{js}} - 1$.

After some manipulations, $A$ in (23) can be expressed as follows

$$A = \Pr\left[\psi g_0 g_m > \theta_2 g_m + 1\right]. \quad (24)$$

where

$$\psi = \min\left\{\begin{array}{l} \frac{\theta_1}{\gamma_0}\left(P_1 - \gamma_0 \sum\limits_{m=2}^{M} P_m\right), \\ \frac{\theta_1}{\gamma_0}\left(P_2 - \gamma_0\left(\varepsilon P_1 + \sum\limits_{3}^{M} P_m\right)\right), \\ \ldots, \frac{\theta_1}{\gamma_0}\left(P_{m-1} - \gamma_0\left(\varepsilon \sum\limits_{l=1}^{m-2} P_l + \sum\limits_{q=m}^{M} P_q\right)\right), \\ , \frac{\theta_1}{\gamma_{th}}\left(P_m - \gamma_{th}\left(\varepsilon \sum\limits_{l=1}^{m-1} P_l + \sum\limits_{q=m+1}^{M} P_q\right)\right) \end{array}\right\}.$$

Because the value of $\psi$ can be positive or negative; hence we consider two cases:

+ In the case of $\psi \leq 0$, $SOP_m$ is given by

$$\begin{aligned} SOP_m &= 1 - A \\ &= 1 - \Pr\left[\underbrace{\psi g_0 g_m}_{\leq 0} > \theta_2 g_m + 1\right] \\ &= 1 - 0 = 1. \end{aligned} \tag{25}$$

+ In the case of $\psi > 0$, $SOP_m$ is given by

$$\begin{aligned} SOP_m &= 1 - \Pr\left[\psi g_0 g_m \geq \theta_2 g_m + 1\right] \\ &= 1 - \Pr\left[g_m \geq \frac{1}{\psi g_0 - \theta_2} \middle| g_0 > \frac{\theta_2}{\psi}\right] \\ &= 1 - \Pr\left[g_m \geq \frac{1}{\psi g_0 - \theta_2} \middle| g_0 \geq \frac{\theta_2}{\psi}\right] \\ &= 1 - \int_{\frac{\theta_2}{\psi}}^{+\infty} \left(1 - F_{g_m}\left(\frac{1}{\psi g_0 - \theta_2}\right)\right) f_{g_0}(x)\, dx \\ &= 1 - \int_{0}^{+\infty} \left(1 - F_{g_m}\left(\frac{1}{\psi t}\right)\right) f_{g_0}\left(t + \frac{\theta_2}{\psi}\right) dt. \end{aligned} \tag{26, 27}$$

*Theorem 1: The SOP at $U_m$ of raw proposed system can be expressed as*

- *In the case of $\psi \leq 0$, the SOP at $U_m$ is equal to 1,*
- *In the case of* $P_m\left(\varepsilon \sum\limits_{l=1}^{m-1} P_l + \sum\limits_{q=m+1}^{M} P_q\right)^{-1} > \gamma_{th}$ *and*

$$\min\left\{\frac{P_1}{\sum\limits_{m=2}^{M} P_m}, \frac{P_2}{\varepsilon P_1 + \sum\limits_{m=3}^{M} P_m}, .., \frac{P_{m-1}}{\varepsilon \sum\limits_{l=1}^{m-2} P_l + \sum\limits_{q=m}^{M} P_q}\right\} > \gamma_0$$

*the SOP at $U_m$ is expressed as*

$$\begin{aligned} SOP_m = 1 - 2 \sum_{j=0}^{N_1-1} \sum_{n_0+..+n_{N_0}} \sum_{m=0}^{\Omega+N_0-1} & \frac{K e^{-\frac{K^*\theta_2}{\psi\lambda_0}} (-1)^{K^*-1}}{\Gamma(N_0)\, \lambda_0^{\Omega+N_0}} \\ & \frac{1}{j!}\left(\frac{1}{\psi\lambda_m}\right)^j \binom{K-1}{n_0, n_1, \ldots, n_{N_0}} \binom{\Omega+N_0-1}{m} \\ & \times \left(\frac{\theta_2}{\psi}\right)^m \\ & \left(\frac{\lambda_0}{\psi\lambda_m K^*}\right)^{w/2} \prod_{0}^{N_0-1} \left(\frac{1}{i!}\right)^{n_{i+1}} \mathcal{F}_{\varpi}\left(2\sqrt{\frac{K^*}{\lambda_0\lambda_m\psi}}\right). \end{aligned} \tag{28}$$

Here, $n_0+n_1+\ldots+n_{N_0} = K-1$, $w = \sum\limits_{i=0}^{N_0-1} i n_{i+1} + N_0 - m - j$, $\Omega = \sum\limits_{i=0}^{N_0-1} i n_{i+1}$, and $K^* = K - n_0$.

*Proof:* See Appendix □

### B. SUM SECRECY RATE (SSR) AND PSO-BASED POWER ALLOCATION FOR THE MAXIMIZATION OF SSR

In the proposed NOMA system, the SSR of the system is defined as the SSR of all destination users at which the secrecy capacity must be satisfied, $R_{\text{sec}}^{U_m} \geq R_{th}$, and SSR can be expressed as

$$R_{\text{sec}} = \sum_{m=1}^{M} R_{\text{sec}}^{U_m} = \sum_{m=1}^{M} \left[\min_{j=1,2,..M}\left\{R_{x_m}^{U_j}\right\} - R_{x_m}^{R_b}\right]^+. \tag{29}$$

Here, $R_{x_m}^{U_j} = \log_2\left(1 + \frac{P_m\theta_1 g_0 g_j}{\left(\varepsilon \sum\limits_{l=1}^{m-1} P_1 + \sum\limits_{q=m+1}^{M} P_q\right)\theta_1 g_0 g_j + \theta_2 g_j + 1}\right)$

and $R_{x_m}^{R_b} = \log_2\left(1 + \frac{P_m g_0}{\left(\sum\limits_{l=1}^{m-1} P_1 + \sum\limits_{q=m+1}^{M} P_q\right) g_0 + P_{js} g_0 + \sigma_{R_b}^2}\right)$

The derivation of the ergodic secrecy rate of the proposed overall system is difficult and is not meaningful for improving the secrecy of the system. Thus, in this section, we focus on the maximization of the SSR based on the power allocation for multiple NOMA users. For any user $U_m$, the secrecy capacity is $R_{\text{sec}}^{U_m} = \left[R_{x_m}^{U_m} - R_{x_m}^{R_b}\right]^+$ with the constraint condition $U_m$ that must successfully decode all stronger signals as $x_1, x_2, \ldots, x_{m-1}$. Therefore, the goal is to maximize the SSR of the proposed NOMA/MIMO system subject to the constraints of the data rates at the users and of the harvested energy at the relay nodes.

The SSR maximization problem can be formulated as follows:

$$\underset{P_1,P_2,...,P_M,P_{js}}{\text{maximize}} \; R_{\text{sec}} = \sum_{1}^{M} \left[\min_{m=2,..M}\left\{R_{x_q}^{U_m}\right\} - R_{x_q}^{R_b}\right]^+ \tag{30}$$

$$\text{s.t. } R_{x_q}^{U_m} \geq R_0 \tag{30a}$$

$$\sum_{m=1}^{M} P_m + P_{js} \leq P_S^{\max} \tag{30b}$$

$$P_1 > P_2 > \ldots > P_m > \ldots > P_M \tag{30c}$$

$$E_{EH}^{PS} \geq e_0. \tag{30d}$$

where $m = 1, 2, 3, \ldots, M$, $q = 1, 2, 3, \ldots, m-1$, $e_0$ is the minimum required harvested energy at the selected UEH relay node, $R_0$ is the minimum required data rate that at

which the users can successfully decode the received stronger signals in the received superimposed signal, and $P_S^{\max}$ is the maximum transmitted power from source $S$.

First, we consider the constraint condition (30a) that is similar to the following conditions

$$\gamma_{x_q}^{U_m} \underset{\substack{m=1,2,3,\ldots,M \\ q=1,\ldots,m-1}}{\geq} \gamma_0. \tag{31}$$

Substituting SINRs from Eqs. (17–20) into Eq. (31) produces the linear constraint conditions for variables $P_m$, $m = 1, .., M$ at any user as described by

$$P_1 \geq \gamma_0 \sum_{m=2}^{M} P_m + \frac{\gamma_0\theta_2}{\theta_1 g_0} + \frac{\gamma_0}{\theta_1 g_0 g_m}, \tag{32a}$$

$$P_2 \geq \gamma_0 \left(\varepsilon P_1 + \sum_{3}^{M} P_m\right) + \frac{\gamma_0\theta_2}{\theta_1 g_0} + \frac{\gamma_0}{\theta_1 g_0 g_m}, \tag{32b}$$

$$\ldots.$$

$$P_{m-1} \geq \gamma_0 \left(\varepsilon \sum_{l=1}^{m-2} P_l + \sum_{q=m}^{M} P_q\right) + \frac{\gamma_0\theta_2}{\theta_1 g_0} + \frac{\gamma_0}{\theta_1 g_0 g_m}. \tag{32c}$$

From (32a, 32b, 32c) we can observe that the inequality $P_m > \frac{\gamma_0\theta_2}{\theta_1 g_0} + \frac{\gamma_0}{\theta_1 g_0 g_m}$, with $m = 1, 2, \ldots, M$ is always true. Therefore, to simplify the problem, we assume that the boundaries for a vector of $M+1$ elements $\{P_1, P_2, \ldots, P_m, \ldots, P_M, P_{js}\}$ are $[\frac{\gamma_0\theta_2}{\theta_1 g_0} + \frac{\gamma_0}{\theta_1 g_0 g_m}, P_S^{max}]$ and $[P_S^{max} - M\left(\frac{\gamma_0\theta_2}{\theta_1 g_0} + \frac{\gamma_0}{\theta_1 g_0 g_m}\right), P_S^{max}]$ for $\{P_1, P_2, \ldots, P_m, \ldots, P_M\}$ and $P_{js}$, respectively.

To solve the problem (30) with multiple constraints, we propose the PSO algorithm [39], [40] which is a stochastic, population-based algorithm modeled on SI that can find a solution for a complex optimization problem. Moreover, the calculation in PSO is very simple and PSO has a better optimization capability compared to the other developing algorithms [41], [48]. The overall algorithm of the global best PSO applied for our proposed system model is presented in **Algorithm 1**, where each individual particle, $k = [1, 2 \ldots, Q]$, where $Q$ is the total number of particles, has a current position $\mathbf{X}_k = \left[P_1, P_2, \ldots, P_m, \ldots, P_M, P_{js}\right]$, a current velocity $\mathbf{V}_k$, a local best position $\mathbf{LB}_k$, and a global best position $\mathbf{GB}_k$ that corresponds to the position where particle $k$ had the highest value as determined by the objective function $f$ for the maximization problem, and a global best position $\mathbf{GB}_k$ that is the highest value among all of the local best $\mathbf{LB}_k$.

In this algorithm, a penalty function is applied to implement the above constraint conditions where we define $b_i$ as the $i$-th constraint ($i = 1, 2, 3, 4$), and $\alpha_i$ is the penalty value. $\varphi(b_i)$ is the satisfaction of the constraint where $\varphi(b_i) = 0$ means that the constraint is satisfied and $\varphi(b_i) = 1$ means that the constraint is not satisfied. Then, based on the objective function, the fitness function can be expressed as

$$f(\mathbf{X}_k) = \sum_{m=1}^{M} \left[\min_{j=1,2,..M} \left\{R_{x_m}^{U_j}\right\} - R_{x_m}^{R_b}\right]^{+} - \sum penalty. \tag{33}$$

where $\sum penalty = \sum_{i=1}^{4} \alpha_i \varphi(b_i)$.

**Algorithm 1** The Global Best PSO Algorithm

**Initialization**:
- Set Constants $Q, C_1, C_2, \xi$
- Initialize the particle positions randomly $\mathbf{X}_k$
- Initialize the particle velocity randomly $\mathbf{V}_k$
- Initialize the local and global best positions: $\mathbf{LB}_k, \mathbf{GB}_k$

**Repeat for loop until the condition is met**:
- *For each particle* $k = [1, 2, \ldots, Q]$
  - Select $r_1^t, r_2^t$ randomly between (0, 1)
  - Update the particle's velocity using Eq.(35a)
  - Update the particle's position using Eq.(35b)
  - Evaluate the best local position:
    - If $f\left(\mathbf{X}_k^{t+1}\right) \geq \mathbf{LB}_k^t$ then $\mathbf{LB}_k^{t+1} = \mathbf{X}_k^{t+1}$
    - If $f\left(\mathbf{X}_k^{t+1}\right) < \mathbf{LB}_k^t$ then $\mathbf{LB}_k^{t+1} = \mathbf{LB}_k^t$
  - Evaluate the best global position:
    - $\mathbf{GB}_k^t = \max\left\{\mathbf{LB}_k^t\right\}$
    - If $f\left(\mathbf{X}_k^t\right) \geq \mathbf{GB}_k$ then $\mathbf{GB}_k = \mathbf{X}_k^t$
- $t \leftarrow t + 1$

**End**: $f(\mathbf{GB}_k)$ as the maximum value of SSR

The following equations define how the local best position is updated at the next time step $t+1$ and the global best position at time step $t$, where $t = [0, .., I_{max}]$, and $I_{max}$ is the maximum number of interactions, respectively:

$$\mathbf{LB}_k^{t+1} = \begin{cases} \mathbf{LB}_k^t iff\left(\mathbf{X}_k^{t+1}\right) < \mathbf{LB}_k^t, \\ \mathbf{X}_k^{t+1} iff\left(\mathbf{X}_k^{t+1}\right) \geq \mathbf{LB}_k^t. \end{cases} \tag{34}$$

here, $\mathbf{GB}_k^t = \max\left\{\mathbf{LB}_k^t\right\}, f\left(\mathbf{X}_k^t\right) \geq \mathbf{GB}_k$ and $\mathbf{GB}_k = \mathbf{X}_k^t$.

Let $\xi$, $C_1$, and $C_2$ denote the inertia weight parameter and cognitive and social parameters, respectively. The velocity and position are updated as

$$\mathbf{V}_k^{t+1} = \xi \mathbf{V}_k^t + C_1 * r_1^t\left(\mathbf{LB}_k^t - \mathbf{X}_k^t\right) + C_2 * r_2^t\left(\mathbf{GB}_k - \mathbf{X}_k^t\right), \tag{35a}$$

$$\mathbf{X}_k^{t+1} = \mathbf{X}_k^t + \mathbf{V}_k^{t+1}. \tag{35b}$$

Here, $r_1^t$ and $r_2^t$ are random numbers between (0,1) at time $t$.

## IV. NUMERICAL RESULTS AND DISCUSSION

### A. THE SECRECY OUTAGE PROBABILITY

In this section, we discuss the theoretical derivations and the Monte Carlo simulations that were performed to validate the analytical expressions for each user given in the previous section; in particular, without a loss of generality, we analyze the simulations results for the MIMO/NOMA with some users such as $U_1$ and $U_2$, and $U_3$ where $U_1$ is located at the longest distance, $U_3$ is located at the nearest distance. Therefore, in considering the two-dimensional plane, the coordinates of the $S$ node, the best relay $R_b$, and users $U_1$, $U_2$, $U_3$ are set to (0, 0), $(x, 0)$, (40, 20), (35, -10), and (30, 11) respectively; here $x = d_0$ (meters). Consequently, the distances of the $R - U_1$, $R - U_2$ links are $d_1 = \sqrt{(40-x)^2 + 20^2}$ (meters), $d_2 = \sqrt{(35-x)^2 + (-10)^2}$

(meters), and $d_3 = \sqrt{(30-x)^2 + 11^2}$ (meters) respectively. In addition, the other parameters in the proposed system are the secrecy target data rate, $R_{th} = 1$ bits/s/Hz, the target data rate is $R_0 = 1$ bits/s/Hz and the path-loss exponent is $m = 2.7$. Moreover, we assume that the value of the noise variance at the relays and users is set as $\sigma^2_{n^a_R} = \sigma^2_{n^c_R} = \sigma^2_{n^a_{U_m}} = -60$ (dBm). Finally, for the secrecy performance comparison with our proposed MIMO/NOMA, in MIMO/OMA, the total bandwidth and transmitted power are shared equally among users.

First, an inspection of all of our figures reveals that the analytical results in the Section III match well with the results of the Monte Carlo simulations. Then, we present a more detailed secrecy performance analysis for each figure, as follows.

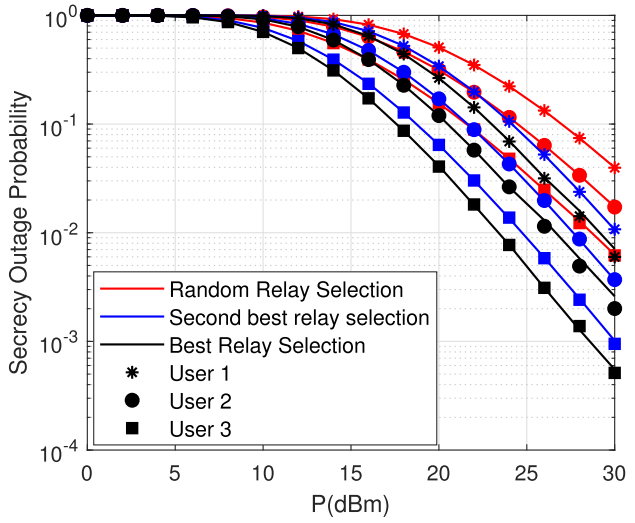


**FIGURE 2.** Effect of relay selection on the SOP.

Figure 2 shows the effects of relay selection based on PRS on the first hop transmission on SOP of our proposed MIMO/NOMA system, and the simulation results are performed for three cases of relay selection in composed of Best Relay Selection, Second best Relay Selection, and Random Relay Selection. The system parameters are set up as: the number of antennas at S and users $N_0 = N_1 = N_2 = N_3 = 3$, the number of relays $K = 3$, $(P_1 = 0.5P, P_2 = 0.2P, P_3 = 0.1P, P_{js} = 0.2P)$, and distance of S-Relay cluster $x = d_0 = 20$. From Figure 2, we can see that the best relay selection method (black curve lines) offers the best secrecy performance among three relay selection approaches while the worst performance occurs with random relay selection (red curve lines). Thus, selecting the best relay node is an optimal solution for relay selection on the first hop.

Figure 3 presents the impacts of the number antennas-relays (a) and 3-users (b) on the secrecy outage performance of our proposed MIMO/NOMA and MIMO/OMA systems in the UEH relaying network. Here, in Figure 3a we consider two cases for the number of antennas at S and the users: (1) S and user equipped single antenna-relay; (2) S and user equipped multiple antenna relays $N_0 = N_1 = N_2 = 3$, $K = 2$. The other parameters are given as $x = d_0 = 20$, $\varepsilon = 1\%$, $\mu = 1$, $\rho = 0.6$, and the power allocation coefficients for both users and the AN signal are respectively $(P_1 = 0.55P, P_2 = 0.25P, P_{js} = 0.2P)$. In Figure 3b, the number of NOMA-user is set up as 3, and $(P_1 = 0.5P, P_2 = 0.2P, P_3 = 0.1P, P_{js} = 0.2P)$, the distance of $R - U_3$ link as $d_3 = 15$(meters). From Figure 3a, it is observed that the secrecy outage performance is enhanced significantly by an increase the number of the antennas at source $S$ and the users. Moreover, Figure 2 shows that the secrecy outage performance of the overall MIMO/NOMA system is better than that of the overall MIMO/OMA system. An examination of Figure 2 shows that for both cases of the number of antenna-relays, the farthest user ($U_1$) shows the lowest secrecy performance whereas the nearest user offers the best performance. This is because due to the NOMA principle, $U_1$ only needs to decode its signal while $U_2$ and $U_3$ must correctly decode the signal of $U_1$, and $(U_1, U_2)$, respectively, and then use SIC to detect its signal. Thus, the decoding of signals $x_2$ and $x_3$ is more difficult than that of signal $x_1$ at $U_1$. Furthermore, it is observed from Figure 3b that the performance difference among the users in the OMA model is higher than that in the NOMA model, $b \sim 2a$, where $b$, $a$ represent the different values of SOP between $U_1$ and $U_3$ for the OMA and NOMA models, respectively. Thus, the NOMA model achieves a better balance in the secrecy performance compared to the OMA model. Finally, we can conclude that our proposed MIMO/NOMA scheme with an UEH relaying network obtains a better secrecy performance compared to the MIMO/OMA system with the MRT and MRC techniques.

Figure 4 displays the effects of power allocations on the secrecy outage probability in both MIMO/NOMA and MIMO/OMA system with MRT/MRC techniques in the UEH relaying network. Here, we investigate the secrecy outage performance for both systems for three cases: $(P_1 = 0.7P, P_2 = 0.15P, P_{js} = 0.15P)$, $(P_1 = 0.6P, P_2 = 0.2P, P_{js} = 0.2P)$ and $(P_1 = 0.55P, P_2 = 0.25P, P_{js} = 0.2P)$. The other parameters are given as $x = d_0 = 20$ (meters), $\varepsilon = 1\%$, $\mu = 1$, and $\rho = 0.5$. First, a glance at Figure 4 reveals that, in this case, the power allocations for each user are related to the secrecy outage performance; hence the curved lines plotted for each user in different cases are changed. It can be observed from Figure 4 that the SOP at each user is different with each value of set power allocation of $(P_1, P_2, P_{js}) = (\alpha_1 P, \alpha_2 P, \alpha_{js} P)$. In particular, in case 1, while the secrecy outage performance at $U_2$ in MIMO/OMA model is better than that in MIMO/NOMA, $U_1$ in the NOMA model offers a higher performance compared to $U_1$ in OMA. However, SOPs at the users in the proposed NOMA are smaller than that in OMA with cases 2 and 3. This is because the power allocation for the jamming signal and for each user are different; hence the secrecy rate in equation (21) is affected, and the secrecy outage performance is also

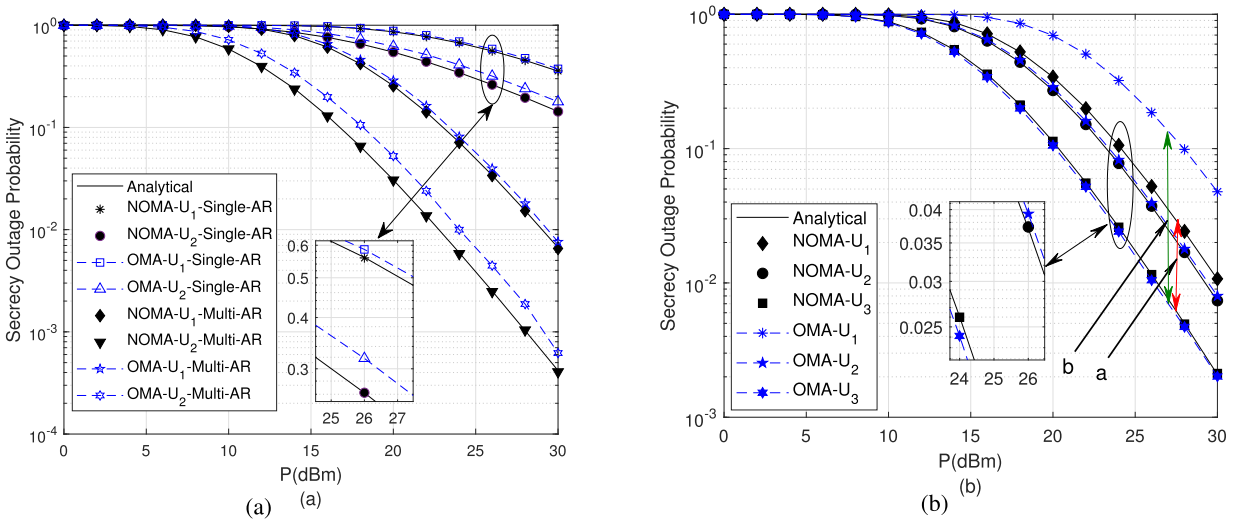


**FIGURE 3.** Effect of the number of Antenna – relays (ARs) (a) and users (b) versus the transmitted power on the SOP.

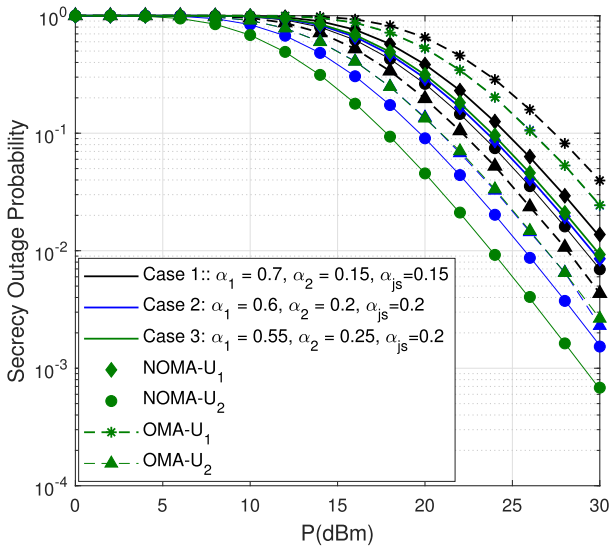


**FIGURE 4.** Effect of different power allocations on the SOP.

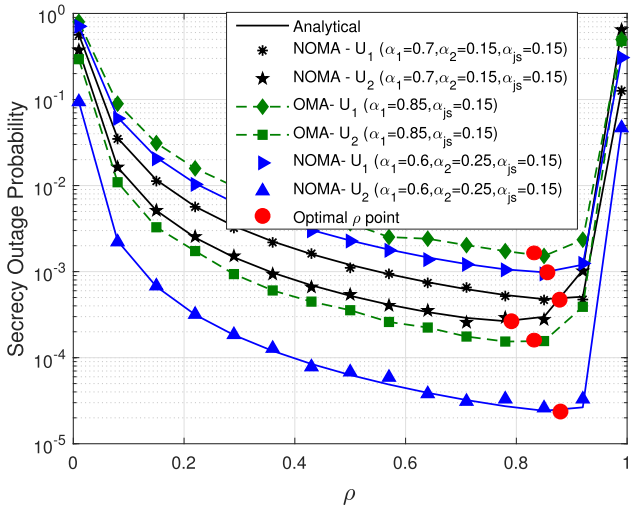


**FIGURE 5.** Effects of the power splitting factor *rho* for PS scheme on the SOP.

impacted; for example, the power of the AN signal increases, leading to a reduction of the SNRs at the UEH relays, and the secrecy data rate increases. In addition, the further user ($U_1$) in the NOMA system obtains a better secrecy performance for all of the considered cases than $U_1$ in the OMA system, demonstrating the benefit of the NOMA principle relative to OMA that the farthest user under the worst channel condition has the highest power. Consequently, the power allocation influences on the SOP of MIMO/NOMA and the selection of this set of parameters is highly important for guaranteeing the secrecy performance of the system.

Figure 5 illustrates the effects of the power splitting factor $\rho$ for the PS scheme on the secrecy outage probability for the proposed model in the UEH relaying network under two cases of the power allocation coefficient set as $(P_1, P_2, P_{js}) = (\alpha_1 P, \alpha_2 P, \alpha_{js} P)$, here $(\alpha_1, \alpha_2, \alpha_{js}) = (0.7, 0.15, 0.15)$ and $(\alpha_1, \alpha_2, \alpha_{js}) = (0.6, 0.25, 0.15)$. The remaining system parameters given in this simulation are similar to those used to obtain the results presented the above figures. First, Figure 5 demonstrates that the secrecy outage probability curves for both users follow the same trend, and shows the optimal value of $\rho$ denoted as $\rho^*$ where the system reaches the highest secrecy outage performance as obtained using the Golden search method [51]; for example, the optimal values are obtained as $\rho^* = 0.8781$ and $\rho^* = 0.7912$ for $U_1$, $U_2$ in NOMA and $\rho^* = 0.7958$ and $\rho^* = 0.8205$ for $U_1$, $U_2$ in OMA, respectively. It is observed that the value of $\rho$ increase from zero to the optimal point and then the SOP decreases to the minimum value; as $\rho$ passes $\rho^*$ the SOP increases to 1, indicating that the secrecy performance is degraded. The cause of this trend is the influence on the SOP of the power splitting factor in the PS protocol; in particular if $\rho$ is small,

the harvested energy at the relay is low; hence, the transmit power at the relay for transmitting signals to the users is small whereas if $\rho$ is high, the small amount of energy is used for signal processing. In addition, it is clear from Figure 5 that with different optimal points are achieved for different power allocations. Furthermore, this figure shows that the secrecy outage performance in the MIMO/NOMA system is superior to that of the MIMO/OMA system.

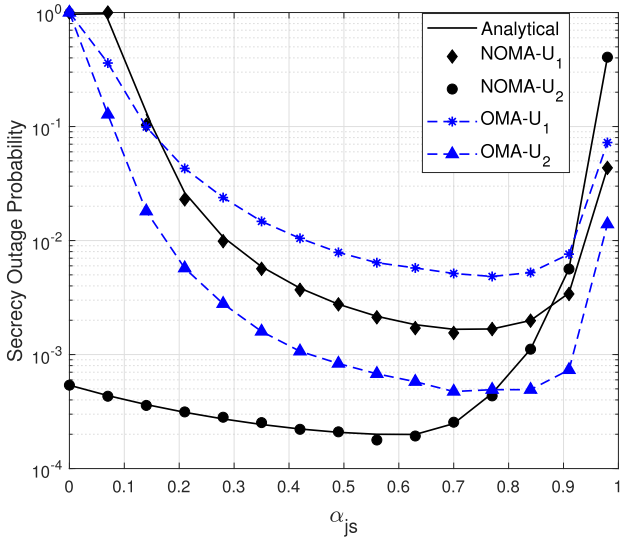


**FIGURE 6.** Effects of the strength of jamming signal on SOP.

Figure 6 presents the impact of power allocation for jamming signal on the SOP of the proposed system in the UEH relay network. In this case, the ratio of the power allocated to $U_1$ and $U_2$ is 0.7/0.3, and the other system parameters are set to be the same for the above results. An examination of Figure 6 shows that the strength of the jamming signal ($\alpha_{js}$) has a significant effect on the secrecy outage performance of both the NOMA and OMA systems. In particular, at very small or very high value of $\alpha_{js}$, the secrecy performance is poor, even in the case where the superimposed source signal without the jamming signal necessary for the secrecy performance is nearly zero ($SOP \rightarrow 1$). Because our proposed model is designed in the UEH relaying network in which the relay node can overhear confidential information. However, if the strength of the jamming signal is too high, the legitimate users' signals are very low; hence the secrecy performance of system is also affected.

Figure 7 presents the influence of the value of the cancellation error term $\varepsilon$ on the SOP versus the transmitter power. The values of the system parameters for this simulation are the same as for the above-described simulations. Here, the secrecy performance of MIMO/OMA is not affected by the cancellation error term and we consider two cases of $\varepsilon = 0.5\%$ and $\varepsilon = 1\%$. At a glance, Figure 7 shows that the SOP is better in the case of small value of $\varepsilon$ and this value affects the secrecy performance at the closer user, $U_2$. Specifically, the secrecy outage performance at $U_2$ of MIMO/NOMA in

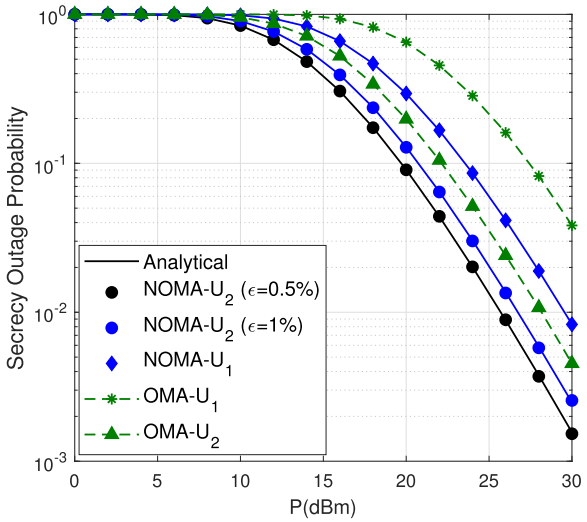


**FIGURE 7.** Effect of imperfect SIC on the SOP.

the case of $\varepsilon = 0.5\%$ is better than that in the case of $\varepsilon = 1\%$. This is due to the effects of the cancellation error term on the decoding of the information of $U_2$; the smaller the value of $\varepsilon$, the more successful the decoding of signal $U_2$. This leads to an increase in the average secrecy capacity at $U_2$. Clearly, the value of the cancellation error term influences the secrecy performance of the system, particularly for $U_2$ in the MIMO/NOMA system.

### B. SSR AND PA-BASED FOR MAXIMIZATION SSR

In this section, we investigate the secrecy performance of our proposed MIMO/NOMA model in the UEH relaying network based on the power allocation using the PSO algorithm. The system parameters such as distances $d_0$, $d_1$, $d_2$, the target secrecy rate, and the noise variance are given as described in Section 4.1. Moreover, for the PSO algorithm we set $C_1 = C_2 = 0.5$, $w = 1$. To illustrate the benefit of the PSO for our proposed model, a comparison with the Exhaustive Search Method is presented. These simulations are implemented using Python and MATLAB software.

Figure 8 shows the convergence as a function of iteration of the PSO algorithm under three different particle sizes (a) and two cases of the target data rate (b). The system parameters are given as the source power $P = 20$ (dBm), the number of antenna-relays $K = 3$, $N_0 = N_1 = N_2 = 3$, $\varepsilon = 0.5\%$, $\rho = 0.8$ and $d_0 = 20, d_1 = 30, d_2 = 20$ (meters). An examination of Figure 8 shows a clear same trend for the curves of the objective function of SSR for all of the cases of the particle size (Figure 8a) and the target data rate (Figure 8b). In particular, the objective function of SSR is enhanced with increasing number of iterations, and the convergence reaches a stable value after approximately 30 iterations; hence the fast convergence of our proposed PSO algorithm for MIMO/NOMA in UEH relaying network is displayed in both Figures 8a and 8b.

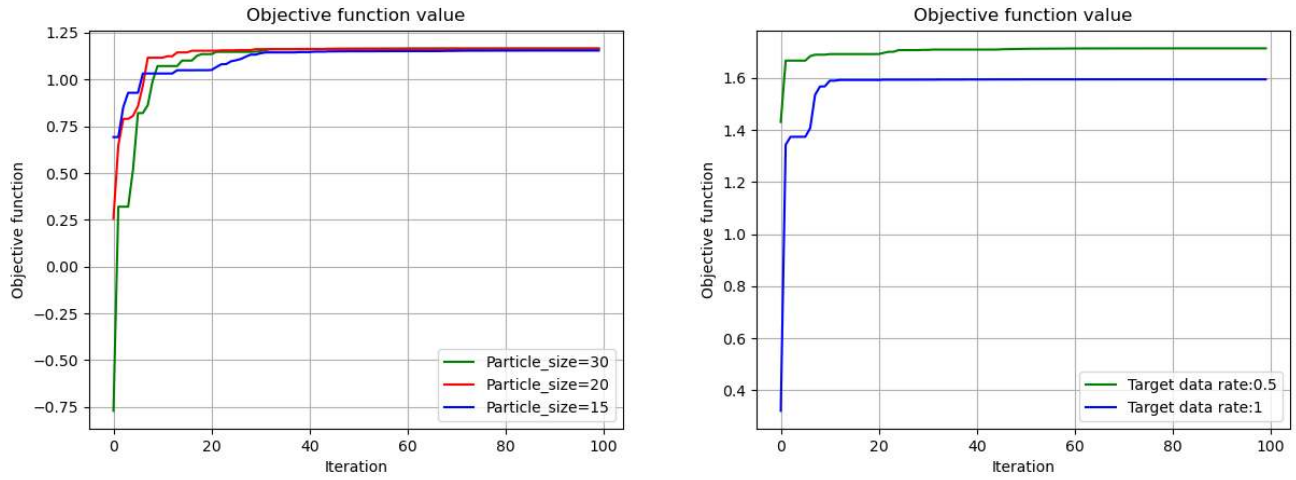


**FIGURE 8.** Convergence behavior of PSO versus Particle size (8a) and the target data rate (8b).

**TABLE 1.** Computation time in the PSO and exhaustive Search methods.

| PSO Method | |
|---|---|
| **Particle Size** | **Computation Time** |
| 30 | 0.0311(s) |
| 20 | 0.0173(s) |
| 15 | 0.0127(s) |
| **Exhaustive Search Method** | |
| **Search Step** | **Computation Time** |
| 0.03 | 2180,7656(s) |
| 0.05 | 191.515(s) |
| 0.1 | 17.935(s) |

Moreover, in addition to convergence behavior, the computation time is also a key factor for the evaluation of the performance of a search approach; hence a comparison of the computation time between the proposed PSO algorithm and exhaustive search algorithm is provided in **Table 1**. This table displays the computation times for both algorithms performed using the same system parameters. An examination of the data presented in **Table 1** shows that the proposed PSO algorithm significantly outperforms the Exhaustive search. In particular, the average time for all of the cases of PSO is approximately $0.0127 - 0.0311$ (s) whereas the computational time in the exhaustive search method is $17,935 - 2180,7656$ (s) for all of the considered search step values (a smaller search step corresponds to higher performance).

Figure 9 shows the maximum secrecy rate of the proposed NOMA system obtained with both exhaustive search and PSO algorithms and the traditional OMA system plotted versus the target data rate ($R_0$). The system parameters are the same as above. It is observed from the figure that the SSR lines for all cases shows the same trend. In particular, when the target data rate increase to approximately 0.9 (bits/s/Hz),

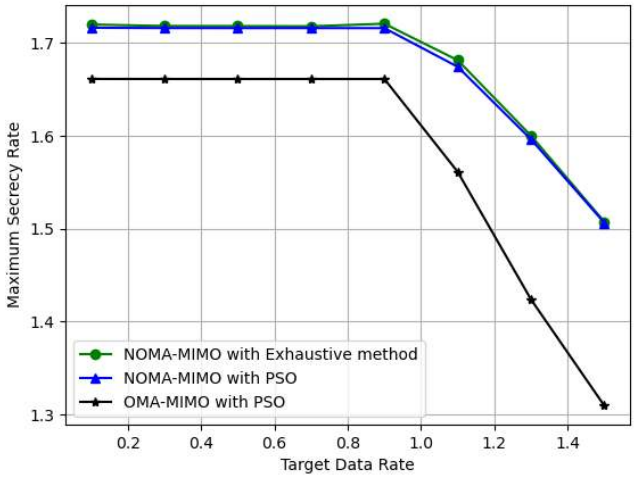


**FIGURE 9.** A comparison of SSR between PSO and Exhaustive algorithms.

the maximum SSR is stable whereas this value decreases dramatically when the target data rate is greater than 0.9 (bits/s/Hz). Clearly, as the threshold of the data rate of the system increases, the achieved secrecy rate in equations (21) and (29) decreases, reducing the maximum value of SSR. Moreover, is is observed that the maximum SSR of the proposed NOMA model is greater than that of the OMA model. Finally, our proposed PSO algorithm for NOMA obtains performance that is close to that of the exhaustive method, while the computation time of the PSO method is much lower than that of the exhaustive search.

Figure 10 shows the effect of energy harvesting efficiency $\mu$ on SSR with some cases of random PA for each user and PA based on the PSO algorithm for our proposed NOMA system. The system parameters are the same as those used for the simulations used to obtain the results shown in Figure 8.

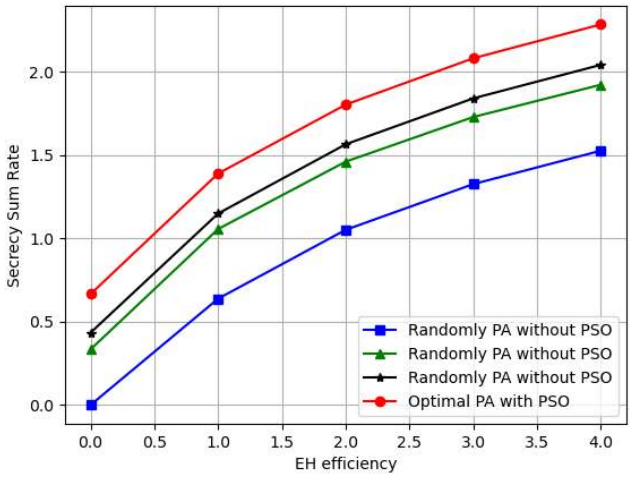


**FIGURE 10.** SSR versus the energy-harvesting efficiency.

A a clear rise in the secrecy sum rate is observed with increasing energy harvesting efficiency. Moreover, a comparison of the four cases presented in Figure 9 shows that the PSO-based algorithm on PA offers the highest SSR whereas the cases of random selection of PA obtain worse performance. This is due to the NOMA principle that the signals are multiplexed by using different power levels based on the channel quality in which the users with poorer channel conditions are allocated more transmission power; hence the optimal power allocation is a key factor for improving the system performance of th eNOMA model.

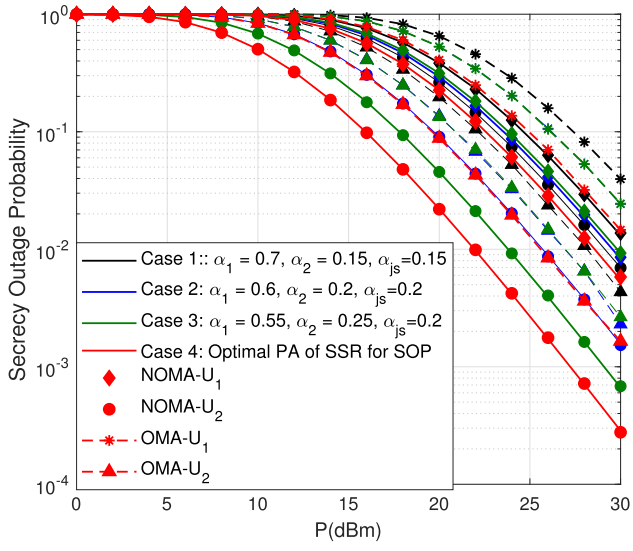


**FIGURE 11.** Effects of the strength of the jamming signal on SOP.

In addition, using the parameters set in the simulations for which the results are shown in Figure 4, Figure 11 investigates the effect of PA on SOP. It is observed from Figure 10 that the optimal PA obtained using the PSO algorithm also affects the secrecy performance. Clearly, in the case of PSO-based on PA applied for optimization of SSR, SOP is also enhanced. In particular, for case 4 (red lines) with the optimal PA, our proposed NOMA system obtains the best secrecy performance for all of the users in comparison with other cases of random PA. Therefore, the optimization of SSR using PSO-based on PA can improve the secrecy outage performance.

## V. CONCLUSION

In this paper, we first considered and analyzed the secrecy outage performance for a MIMO/NOMA system using MRT/MRC in an untrusted EH relaying network with the PS protocol over a Rayleigh fading channel. Moreover, to improve the secrecy performance of the proposed system, we used the PSO algorithm based on PA to maximize SSR. In our proposed model, the source and users are equipped with multiple-antennas while the untrusted EH relaying node with single-antenna plays two roles: (i) the helper forwards the signal from $S$ to users, and (ii) the eavesdropper can overhear the confidential information of both users. To enhance the secrecy performance of our proposed system, the source $S$ with a jammer simultaneously transmits the AN jamming signal to interfere with eavesdroppers. Moreover, the analytical expression of the SOP at each user was derived. Finally, a Monte Carlo simulation was used to validate these analytical results. To obtain a better understanding of the effectiveness of the MIMO/NOMA system, a comparison between the MIMO/NOMA and MIMO/OMA systems was provided in our analysis results. Moreover, the impacts of various system parameters, such as the number of antenna and relay nodes, the power allocation coefficients, power-splitting ratio, successive interference cancellation (SIC), and the energy-harvesting efficiency on the system performance were investigated. Finally, theoretical and simulation results showed the following: (i) the benefits of increasing the number of antennas and relay nodes; (ii) the choice of the power allocation coefficient and AN signal affects the secrecy performance of the system; (iii) the operation of SIC influences the secrecy performance of the system, such that a smaller cancellation error term leads to a higher secrecy performance; (iv) the selection of a suitable PS factor in the EH model will improve the secrecy performance of the system using the Golden Search Method; (v) using PSO-based PA will enhance the secrecy performance of the proposed system in both SOP and SSR; and (v) in all scenarios, the MIMO/NOMA offers a better secrecy performance than the MIMO/OMA system.

## APPENDIX

This appendix derives the SOP at $U_m$ for our proposed NOMA/MIMO system with imperfect SIC using the cluster of UEH relaying nodes in the network.

By substituting (2b) and (3a) into (27), Equation in (27) can be rewritten as follows:

$$SOP_m = 1 - \frac{K e^{-\frac{\theta_2}{\psi \lambda_0}}}{\Gamma(N_0)\,\lambda_0^{N_0}} \mathbf{I}_1. \tag{36}$$

Here,

$$\mathbf{I}_1 = \int_0^{+\infty} \left[ e^{-\frac{1}{\psi\lambda_m t}-\frac{t}{\lambda_0}} \sum_{j=0}^{N_m-1} \frac{1}{j!}\left(\frac{1}{\psi\lambda_m t}\right)^j \left(t+\frac{\theta_2}{\psi}\right)^{N_0-1} \left(1-e^{-\frac{t}{\lambda_0}-\frac{\theta_2}{\psi\lambda_0}} \sum_{j=0}^{N_0-1} \frac{1}{j!}\left(\frac{t}{\lambda_0}+\frac{\theta_2}{\psi\lambda_0}\right)^j\right)^{K-1}\right] dt \tag{37}$$

Applying equation [ [49], Eq. 26.4.10] as following equation

$$(x_1+x_2+\ldots+x_k)^n = \sum \binom{n}{n_1,n_2,\ldots,n_k} x_1^{n_1}x_2^{n_2}\ldots x_k^{n_k}. \tag{38}$$

where the summation is over all nonnegative integers $n_1, n_2, \ldots, n_k$ such that $n_1+n_2+\ldots+n_k = n$.

Let us denote $w = \sum_{i=0}^{N_0-1} in_{i+1} + N_0 - m - j$, $\Omega = \sum_{i=0}^{N_0-1} in_{i+1}$, and $K^* = K - n_0$; hence, $\mathbf{I}_1$ in (37) can be formulated as

$$\mathbf{I}_1 = \sum_{j=0}^{N_m-1} \sum_{(n_0+n_1+\ldots+n_{N_0})} \binom{K-1}{n_0,n_1,\ldots,n_{N_0}} \frac{e^{-(K^*-1)\frac{\theta_2}{\psi\lambda_0}}}{j!\lambda_0^{\sum_{i=0}^{N_0-1} in_{i+1}}} \left(\frac{1}{\psi\lambda_m}\right)^j (-1)^{K^*-1} \prod_{i=0}^{N_0-1}\left(\frac{1}{i!}\right)^{n_{i+1}} \mathbf{I}_2. \tag{39}$$

where,

$$\mathbf{I}_2 = \int_0^{+\infty} e^{-\frac{1}{\psi\lambda_m t}-\frac{tK^*}{\lambda_0}} \left(\frac{1}{t}\right)^j \left(t+\frac{\theta_2}{\psi}\right)^{\Omega+N_0-1} dt. \tag{40}$$

Applying the Newton binomial $(a+b)^k = \sum_{i=0}^{k} \binom{k}{i} a^{k-i}b^i$, $\mathbf{I}_2$ can be expressed as

$$\mathbf{I}_2 = \int_0^{+\infty} e^{-\frac{1}{\psi\lambda_m t}-\frac{tK^*}{\lambda_0}} \left(\frac{1}{t}\right)^j \sum_{m=0}^{\Omega+N_0-1} \binom{\Omega+N_0-1}{m} \times t^{w+j}\left(\frac{\theta_2}{\psi}\right)^m dt \tag{41}$$

By using [ [50], Eq.(3.471.9)] $\int_0^{\infty} x^{v-1}e^{-\frac{\beta}{x}-\gamma x}dx = 2\left(\frac{\beta}{\gamma}\right)^{\frac{v}{2}} K_v\left(2\sqrt{\beta\gamma}\right)$, $Re(\beta) > 0$ and $Re(\gamma) > 0$ we obtain $SOP_m$ as in (28). This completes the proof of Theorem 1.

## REFERENCES


[1] K. David and H. Berndt, "6G vision and requirements: Is there any need for beyond 5G?" *IEEE Veh. Technol. Mag.*, vol. 13, no. 3, pp. 72–80, Sep. 2018.

[2] A. U. Gawas, "An overview on evolution of mobile wireless communication networks: 1G-6G," *Int. J. Recent Innov. Trends Comput. Commun.*, vol. 3, no. 5, pp. 3130–3133, 2015.

[3] M. Giordani, M. Polese, M. Mezzavilla, S. Rangan, and M. Zorzi, "Towards 6G networks: Use cases and technologies," 2019, *arXiv:1903.12216*. [Online]. Available: http://arxiv.org/abs/1903.12216

[4] H. Yang, A. Alphones, Z. Xiong, D. Niyato, J. Zhao, and K. Wu, "Artificial intelligence-enabled intelligent 6G networks," 2019, *arXiv:1912.05744*. [Online]. Available: http://arxiv.org/abs/1912.05744

[5] Z. Ding, Y. Liu, J. Choi, Q. Sun, M. Elkashlan, I. Chih-Lin, and H. V. Poor, "Application of non-orthogonal multiple access in LTE and 5G networks," *IEEE Commun. Mag.*, vol. 55, no. 2, pp. 185–191, Feb. 2017.

[6] O. Maraqa, A. S. Rajasekaran, S. Al-Ahmadi, H. Yanikomeroglu, and S. M. Sait, "A survey of rate-optimal power domain NOMA with enabling technologies of future wireless networks," *IEEE Commun. Surveys Tuts.*, vol. 22, no. 4, pp. 2192–2235, 2nd Quart., 2020.

[7] M. Bloch, J. Barros, M. R. Rodrigues, and S. W. McLaughlin, "Wireless information-theoretic security," *IEEE Trans. Inf. Theory*, vol. 54, no. 6, p. 2515–2534, Dec. 2008.

[8] X. Chen, D. Wing Kwan Ng, W. Yu, E. G. Larsson, N. Al-Dhahir, and R. Schober, "Massive access for 5G and beyond," 2020, *arXiv:2002.03491*. [Online]. Available: http://arxiv.org/abs/2002.03491

[9] S. Singh, D. Mitra, and R. K. Baghel, "Analysis of NOMA for future cellular communication," in *Proc. 3rd Int. Conf. Trends Electron. Informat. (ICOEI)*, Apr. 2019, pp. 389–395.

[10] A. Islam and K. Dobre, "Power-domain non-orthogonal multiple access (NOMA) in 5G systems: Potentials and challenges," *IEEE Commun. Surveys Tuts.*, vol. 19, no. 2, p. 721–742, 4th Quart., 2017.

[11] M. Liaqat, K. A. Noordin, T. Abdul Latef, and K. Dimyati, "Power-domain non orthogonal multiple access (PD-NOMA) in cooperative networks: An overview," *Wireless Netw.*, vol. 26, no. 1, pp. 181–203, Jan. 2020.

[12] D. Wan, M. Wen, F. Ji, H. Yu, and F. Chen, "Non-orthogonal multiple access for cooperative communications: Challenges, opportunities, and trends," *IEEE Wireless Commun.*, vol. 25, no. 2, pp. 109–117, Apr. 2018.

[13] X. Liang, Y. Wu, S. Kwan Ng, Y. Zuo, S. Jin, and H. Zhu, "Outage performance for cooperative NOMA transmission with an AF relay," *IEEE Commun. Lett.*, vol. 21, no. 11, pp. 2428–2431, Nov. 2017.

[14] T. A. Le and H. Y. Kong "Energy harvesting relay-antenna selection in cooperative MIMO/NOMA network over Rayleigh fading," *Wireless Netw.*, vol. 26, p. 2075–2087, Dec. 2020.

[15] Z. Shi, W. Gao, S. Zhang, J. Liu, and N. Kato, "AI-enhanced cooperative spectrum sensing for non-orthogonal multiple access," *IEEE Wireless Commun.*, vol. 27, no. 2, pp. 173–179, Apr. 2020.

[16] L. Lv, J. Chen, Q. Ni, Z. Ding, H. Jiang, and S. Sharing, "Cognitive non-orthogonal multiple access with cooperative relaying: A new wireless frontier for 5g spectrum sharing," *IEEE Commun. Mag.*, vol. 56, no. 4, pp. 188–195, Apr. 2018.

[17] Y. Liu, H. Xing, C. Pan, A. Nallanathan, M. Elkashlan, and L. Hanzo, "Multiple-antenna-assisted non-orthogonal multiple access," *IEEE Wireless Commun.*, vol. 25, no. 2, pp. 17–23, Apr. 2018.

[18] M. Zeng, A. Yadav, O. A. Dobre, G. I. Tsiropoulos, and H. Vincent Poor, "Capacity comparison between MIMO-NOMA and MIMO-OMA with multiple users in a cluster," 2017, *arXiv:1706.02731*. [Online]. Available: http://arxiv.org/abs/1706.02731

[19] Paradiso and Starner, "Energy scavenging for mobile and wireless electronics," *IEEE Pervas. Comput.*, vol. 4, no. 1, pp. 18–27, Jan./Mar. 2005.

[20] L. Varshney, "Transporting information and energy simultaneously," in *Proc. ISIT*, 2008, pp. 1612–1616.

[21] L. Liu, R. Zhang, and K.-C. Chua, "Wireless information transfer with opportunistic energy harvesting," *IEEE Trans. Wireless Commun.*, vol. 12, no. 1, pp. 288–300, Jan. 2013.

[22] M. Ashraf, J.-W. Jang, J.-K. Han, and K. G. Lee, "Capacity maximizing adaptive power splitting protocol for cooperative energy harvesting communication systems," *IEEE Commun. Lett.*, vol. 22, no. 5, pp. 902–905, May 2018.

[23] M. A. Abd-Elmagid, T. ElBatt, and K. G. Seddik, "Optimization of energy-constrained wireless powered communication networks with heterogeneous nodes," *Wireless Netw.*, vol. 25, no. 2, pp. 713–730, Feb. 2019.

[24] K. Wu, F. Li, C. Tellambura, and H. Jiang, "Optimal selective transmission policy for energy-harvesting wireless sensors via monotone neural networks," *IEEE Internet Things J.*, vol. 6, no. 6, pp. 9963–9978, Dec. 2019.

[25] D. Nasir, "Relaying protocols for wireless energy harvesting and information processing," *IEEE Trans. Wireless Commun.*, vol. 12, no. 7, pp. 3622–3636, Jul. 2013.

[26] Y. Liu, H. Ding, J. Shen, R. Xiao, and H. Yang, "Outage performance analysis for SWIPT-based cooperative non-orthogonal multiple access systems," *IEEE Commun. Lett.*, vol. 23, no. 9, pp. 1501–1505, Sep. 2019.

[27] Kader, Md Fazlul, "Cooperative non-orthogonal multiple access with SWIPT over Nakagami-m fading channels," *Trans. Emerg. Telecommun. Technol.*, vol. 30, no. 5, e3571, 2019.
[28] A. A. Nasir, H. D. Tuan, T. Q. Duong, and M. Debbah, "NOMA throughput and energy efficiency in energy harvesting enabled networks," *IEEE Trans. Commun.*, vol. 67, no. 9, pp. 6499–6511, Dec. 2019.
[29] J. Tang, J. Luo, M. Liu, D. K. C. So, E. Alsusa, G. Chen, K.-K. Wong, and J. A. Chambers, "Energy efficiency optimization for NOMA with SWIPT," *IEEE J. Sel. Topics Signal Process.*, vol. 13, no. 3, pp. 452–466, Jun. 2019.
[30] B. Qiu and C. Jing, "Performance analysis for cooperative jamming and artificial noise aided secure transmission scheme," *Veh. Commun. Netw.*, Dec. 2020. [Online]. Available: https://www.researchsquare.com/article/rs-45614/v1, doi: 10.21203/rs.3.rs-45614/v1.
[31] Y. Gu, Z. Wu, Z. Yin, and X. Zhang, "The secrecy capacity optimization artificial noise: A new type of artificial noise for secure communication in MIMO system," *IEEE Access*, vol. 7, pp. 58353–58360, 2019.
[32] H. Lei, Z. Yang, K. Park, I. Ansari, Y. Guo, G. Pan, and M. Alouini, "Secrecy outage analysis for cooperative NOMA systems with relay selection schemes," *IEEE Trans. Commun.*, vol. 67, no. 9, pp. 6282–6298, Dec. 2019.
[33] T. A. Le and H. Y. Kong, "Secrecy analysis of a cooperative NOMA network using an EH untrusted relay," *Int. J. Electron.*, vol. 106, no. 6, pp. 799–815, Jun. 2019.
[34] V. N. Vo, C. So-In, H. Tran, D.-D. Tran, S. Heng, P. Aimtongkham, and A.-N. Nguyen, "On security and throughput for energy harvesting untrusted relays in IoT systems using NOMA," *IEEE Access*, vol. 7, pp. 149341–149354, 2019.
[35] J. Yan, Q. Li, Q. Zhang, L. Yang, and J. Qin, "Secrecy sum rate optimization in MISO non-orthogonal multiple access systems with orthogonal space-time block coding," *Int. J. Commun. Syst.*, vol. 33, no. 1, p. e4132, 2020.
[36] W. Yu, A. Chorti, L. Musavian, H. V. Poor, and Q. Ni, "Effective secrecy rate for a downlink NOMA network," *IEEE Trans. Wireless Commun.*, vol. 18, no. 12, pp. 5673–5690, Dec. 2019.
[37] H. Zhang, B. Wang, C. Jiang, K. Long, A. Nallanathan, V. C. M. Leung, and H. V. Poor, "Energy efficient dynamic resource optimization in NOMA system," *IEEE Trans. Wireless Commun.*, vol. 17, no. 9, pp. 5671–5683, Feb. 2018.
[38] G. He, L. Li, X. Li, W. Chen, L. L. Yang, and Z. Han, "Secrecy sum rate maximization in NOMA systems with wireless information and power transfer," in *Proc. 9th Int. Conf. Wireless Commun. Signal Process.*, 2017, pp. 1–6.
[39] K. Y. Lee and M. A. El-Sharkawi, "Modern heuristic optimization techniques with applications to power systems," in *Proc. IEEE Power Eng. Soc.*, 2002, p. 02TP160, 2002.
[40] Z.-L. Gaing, "Particle swarm optimization to solving the economic dispatch considering the generator constraints," *IEEE Trans. Power Syst.*, vol. 18, no. 3, pp. 1187–1195, Aug. 2003.
[41] Y. Shi and R. C. Eberhart, "Comparison between genetic algorithms and particle swarm optimization," in *Proc. 7th Int. Conf. Evol. Program.*, Mar. 1998, pp. 611–616.
[42] S. Hak Gupta, R. K. Singh, and S. N. Sharan, "An approach to implement PSO to optimize outage probability of coded cooperative communication with multiple relays," *Alexandria Eng. J.*, vol. 55, no. 3, pp. 2805–2810, Sep. 2016.
[43] A. Masaracchia, D. B. Da Costa, T. Q. Duong, M.-N. Nguyen, and M. T. Nguyen, "A PSO-based approach for user-pairing schemes in NOMA systems: Theory and applications," *IEEE Access*, vol. 7, pp. 90550–90564, 2019.
[44] J. Chen, S. Huang, H. Li, X. Lv, and Y. Cai, "PSO-based agent cooperative spectrum sensing in cognitive radio networks," *IEEE Access*, vol. 7, pp. 142963–142973, 2019.
[45] R. Wan, L. Zhu, T. Li, and L. Bai, "A NOMA-PSO based cooperative transmission method in satellite communication systems," in *Proc. 9th Int. Conf. Wireless Commun. Signal Process. (WCSP)*, Oct. 2017, pp. 1–6.
[46] A. D. Wyner, "The wire-tap channel," *Bell Syst. Tech. J.*, vol. 54, no. 8, pp. 1355–1387, Oct. 1975.
[47] M. Bloch, J. Barros, M. R. Rodrigues, and S. W. McLaughlin, "Wireless information theoretic security," *IEEE Trans. Inf. Theory*, vol. 54, no. 6, p. 2515–2534, May 2008.
[48] V. Selvi and D. R. Umarani, "Comparative analysis of ant colony and particle swarm optimization techniques," *Int. J. Comput. Appl.*, vol. 5, no. 4, pp. 1–6, Aug. 2010.
[49] R. Gradshteyn, *Table of intergrals, series, and Products*. New York, NY, USA: Academic, 2014.
[50] F. W. J. Olver, D. W. Lozier, R. F. Boisvert, and C. W. Clark, *NIST Handbook of Mathematical Functions*. New York, NY, USA: Cambridge Univ. Press, 2010.
[51] W. H. Teukolsky, "Section 10.2. Golden section search in one dimension," in *Numerical Recipes: The Art of Scientific Computing*. New York, NY, USA: Cambridge Univ. Press, 2007, pp. 492–496.

**LE THI ANH** received the B.E. degree in electrical engineering and the M.E. degree in information system from Le Quy Don Technical University, Vietnam, in 2011 and 2015, respectively, and the Ph.D. degree from the Department of Electrical Engineering, University of Ulsan, South Korea, in 2020. She is currently a Postdoctoral Research Fellow with Kongju National University, South Korea. Her major research interests are cooperative NOMA communications systems, MIMO communication, physical-layer security, and energy harvesting.

**IC PYO HONG** (Member, IEEE) received the B.S., M.S., and Ph.D. degrees in electronics engineering from Yonsei University, Seoul, South Korea, in 1994, 1996, and 2000, respectively. From 2000 to 2003, he was with the Information and Communication Division, Samsung Electronics Company, Suwon, South Korea, where he was a Senior Engineer with the CDMA Mobile Research. Since 2003, he has been with the Department of Information and Communication Engineering, Kongju National University, Cheonan, South Korea. In 2006, he was a Visiting Scholar with Texas A&M University, College Station, TX, USA. In 2012, he was also a Visiting Scholar with Syracuse University, Syracuse, NY, USA. He is currently a Professor with Kongju National University. His research interests include the use of numerical techniques in electromagnetic and periodic electromagnetic structures.